

Supporting Information

FUNCTIONALIZED MESOPOROUS SOLIDS BASED ON MAGADIITE AND [Al]-MAGADIITE

Hipassia M. Moura and Heloise O. Pastore*

Institute of Chemistry, University of Campinas, 270 Monteiro Lobato St, 13083 861, Campinas/São Paulo, Brazil.

* Corresponding author. Phone: +55-19-35213095; E-mail: gpmmm@iqm.unicamp.br

Experimental details. Synthesis and characterization.

Table S1. Chemical analyses of CTA-magadiites and CTA-[Al]-magadiites.

Table S2. Interlayer space of modified magadiites.

Table S3. Unit cell and $\text{Si}_T/(\text{Si}_T + \text{Si}_Q)$ ratios of the ^{29}Si sites on the final solids.

Table S4. Specific surface area (S_{BET}), pore volume (V) and pore diameter (D) of the HYB-magaX and HYB-[Al]-magaX.

Table S5. Results of CO_2 adsorption in modified magadiite and [Al]-magadiite.

Figure S1. X-ray diffractograms of (A): a) magadiite, b) CTA-maga28, c) CTA-maga61, d) CTA-maga88 and e) CTA-maga100. (B): a) [Al]-magadiite, b) CTA-[Al]-maga39, b) HYB-[Al]-maga39, c) CTA-[Al]-maga63, d) CTA-[Al]-maga72 and e) CTA-[Al]-maga99.

Figure S2. Position of CTA^+ chain in relation to the lamella (magadiite lamella thickness = 1.12 nm).

Figure S3. FT-IR spectra of hybrid materials derivated from magadiite and [Al]-magadiites.

Figure S4. ^{13}C SS-NMR spectra of hybrid materials derivated from magadiite and [Al]-magadiites.

Figure S5. Scanning Electronic Microscopy (SEM) of hybrid materials based on [Al]-magadiite.

Figure S6. Surface area (■) and pore volume (□) as a function of CTA/Na in magadiite (A) and [Al]-magadiite (B).

EXPERIMENTAL SECTION

Pillarization process. The pillarizing process occurred by the method proposed by Zhu *et al.*¹ and used previously for magadiite.² A solution of hydrolyzed TEOS in ethanol was added to the organomodified-magadiite suspensions (1 wt.%) and stirred for 3h at room temperature. The mixture was transferred to a stainless steel autoclave lined with Teflon for the hydrothermal treatment for 66h at 100°C. The solids were calcined at 550 °C for 10h under O₂ atmosphere. The samples were named PILC-[Al]-magaX (where X corresponds to the CTA/Na molar percentage on the starting magadiite).

Grafting process. The grafting process was performed as described in the literature by Wang *et al.*³. Approximately 0.25g of CTA-magaX/CTA-[Al]-magaX was dried in an oven for 24h at 100°C and after added to 125 mL of dried N-dimethylacetamide (DMAC) and stirred for 4h under Ar atmosphere at room temperature. Subsequently, γ -aminopropyltriethoxysilane was added to this mixture and stirred for 48h at 70°C under reflux and inert atmosphere. The final solid was washed with DMAC and dried. The solids were labeled γ -magaX and γ -[Al]-magaX (where X corresponds to the CTA/Na molar percentage on the starting magadiite).

Characterization. Confirmation of the formation of desired materials was made by X-ray diffraction (XRD) in XRD7000 Shimadzu apparatus with Cu radiation ($K_{\alpha 1} = 1.5406 \text{ \AA}$). Slits of 5 mm were used for dispersion and convergence and 3° for exiting radiation. Measurements were obtained in the region from 1.4 to 55° (2 θ). The basal spacing and distances were calculated by Bragg's equation ($n\lambda = 2d\sin\theta$). Field Emission Scanning Electron Microscopy (FE SEM) data were obtained in a JEOL JSM6340. The samples were prepared over a carbon film and coated with gold:palladium (80:20%). For Transmission Electron Microscopy (TEM) and Selected Area Electron Diffraction (SAED) images, the sample was dispersed in distilled water and applied to 400-mesh copper grid coated with parlodio/carbon. The imaging was performed at Zeiss Microscope Libra 120 with CCD Olympus i-TEM Cantege camera. The elemental analyses of carbon, hydrogen and nitrogen were obtained from CHNS/O Analyzer 2400 series II from Perkin Elmer. The Na and Al contents were determined by ICP-OES. The solids were calcined at 900 °C and dissolved in 3 mL of HF (Aldrich 48%), 3 mL of HNO₃ (Aldrich 65 wt.%) and three drops of HClO₄ (Mallinckrodt, 70 wt.%) in a sand bath, at 200 °C. After nearly complete evaporation of acids, small amounts of boric acid were added to the complete the elimination of HF. Solutions of these samples were prepared in HNO₃ solution 1.0 wt.% and analysed in a Optmar 3000 DV Perkin Elmer equipment. The structural order at short distances was analyzed by Fourier-transformed infrared spectroscopy (FTIR) using KBr pellets (0.5 wt%) in a Nicolet 6700 spectrophotometer at a resolution of 4 cm⁻¹ and with accumulation of 32 scans. Solid-State Nuclear Magnetic Resonance was used to probe the nucleus at short distances. High Power Decoupling (HPDEC) NMR spectra were measured for ²⁷Al and ²⁹Si in a Bruker Avance400+ II. The samples were spun at 10kHz in a zirconia rotor. More than 1024 scans were obtained for proton-decoupled ²⁹Si NMR, with 60 s delay time and tetramethylsilane (TMS) as reference. For proton-decoupled ²⁷Al, more than 2000 scans were accumulated at 0.5 s

delay time and an aqueous acid solution of $\text{Al}(\text{NO}_3)_3$ was the reference at 0 ppm. For $^{13}\text{C}\{-^1\text{H}\}$ CP MAS NMR spectra, adamantane ($\text{C}_{10}\text{H}_{16}$) was used as reference. ^{29}Si liquid state nuclear magnetic resonance was measured in a Bruker Avance500 where a 5 mm glass tube was used. The measurements were performed using a D_2O capillary, 7200 scans were accumulated at 30 s delay time. The N_2 adsorption/desorption isotherms were obtained by nitrogen adsorption at cryogenic temperature in a NOVA 4200e equipment (Quantachrome Instruments). The samples were heated at 100°C under vacuum for 24h prior to the measurement. Surface areas were determined using the Brunauer-Emmett-Teller (BET) method and pore size distribution data were collected by the NLDFT method using cylindrical pores on silica. Temperature-programmed desorption (TPD) experiments were performed on a Quantachrome CHEMBET-3000 TPD/TPR instrument equipped with a TC detector. Approximately 100 mg of sorbent was placed in a U-shaped quartz reactor, heated to 150°C at a rate of $10^\circ\text{C min}^{-1}$ and held at this temperature for 3 h under He flow (30 mL min^{-1}) to eliminate water and adsorbed gases. Then, the temperature was reduced to 50°C and CO_2 (5 vol. % in He) flow (20 mL min^{-1}) contacted the sorbent for 2 h (adsorption temperature and time were determined previously). After that, the sample was submitted to He flow (20 mL min^{-1}) for 1h and temperature decreased to 30°C . The CO_2 desorption was carried out between $30\text{-}150^\circ\text{C}$ a rate $10^\circ\text{C min}^{-1}$ and the CO_2 adsorption capacity was calculated on the basis of desorption by external calibration method.

Table S1. Chemical analysis of CTA-magadiites and CTA-[Al]-magadiites.

	CTA ⁺ /Na ⁺ calculated	Water (%) ^a	C (%) ^b	N (%) ^b	CTA ⁺ /Na ⁺ final solid ^b	Unit Cell
Magadiita	0%	14.98	0.14	0.01	-	Na ₂ Si ₁₄ O ₂₉ · 8.0H ₂ O
	25%	6.1	10.33	0.63	28%	Na _{1.44} CTA _{0.56} Si ₁₄ O ₂₉ · 4.0H ₂ O
	50%	4.5	20.16	1.21	61%	Na _{0.78} CTA _{1.22} Si ₁₄ O ₂₉ · 3.2H ₂ O
	75%	3.5	25.16	1.56	88%	Na _{0.24} CTA _{1.76} Si ₁₄ O ₂₉ · 2.7H ₂ O
	100%	3.4	30.58	1.85	108%	CTA ₂ Si ₁₄ O ₂₉ · 2.7H ₂ O
[Al]-magadiita	0%	17.0	0.11	0.01	-	Na ₂ Al _{0.95} Si _{13.05} O ₂₉ · 10H ₂ O
	25%	4.5	15.05	0.88	39%	Na _{1.77} CTA _{1.23} Al _{0.95} Si _{13.05} O ₂₉ · 3.4H ₂ O
	50%	3.4	19.47	1.22	63%	Na _{1.17} CTA _{1.83} Al _{0.95} Si _{13.05} O ₂₉ · 2.7H ₂ O
	75%	3.5	20.85	1.29	72%	Na _{0.84} CTA _{2.16} Al _{0.95} Si _{13.05} O ₂₉ · 2.9H ₂ O
	100%	3.9	22.16	1.55	99%	CTA ₂ Al _{0.95} Si _{13.05} O ₂₉ · 3.0H ₂ O

a) By TG and b) by chemical analyses (CHN)

Table S2. Interlayer space of modified magadiites.

Sample	Peak position/ °2θ/ Distance/ nm	Sample	Peak position/°2θ/ Distance/ nm
Magadiite	5.76/1.53	[Al]-magadiite	5.74/1.54
CTA-Maga28	2.80/3.15	CTA-[Al]-maga39	2.81/3.14
HYB-maga28	6.38/1.38	HYB-[Al]-maga39	6.24/1.42
HYB-maga61	6.28/1.41	HYB-[Al]-maga63	4.98/1.77
HYB-maga88	5.93/1.49	HYB-[Al]-maga72	5.48/1.61
HYB-maga100	5.69/1.55	HYB-[Al]-maga99	5.58/1.58

Table S3. Unit cell and $\text{Si}_T/(\text{Si}_T + \text{Si}_Q)$ ratios of the ^{29}Si sites on the final solids.

	% Si (T) = $\text{Si}_T/(\text{Si}_T + \text{Si}_Q)$	Unit cell*
HYB-maga28	26.0	$(\text{Na}_2\text{O})(\text{Si}(\text{CH}_2)_3\text{NH}_2)_{72.5}(\text{SiO}_2)_{206.5}$
HYB-maga61	27.7	$(\text{Na}_2\text{O})(\text{Si}(\text{CH}_2)_3\text{NH}_2)_{225.5}(\text{SiO}_2)_{588.5}$
HYB-maga88	31.0	$(\text{Na}_2\text{O})(\text{Si}(\text{CH}_2)_3\text{NH}_2)_{148.5}(\text{SiO}_2)_{330.5}$
HYB-maga100	25.0	$(\text{Na}_2\text{O})(\text{Si}(\text{CH}_2)_3\text{NH}_2)_{74.9}(\text{SiO}_2)_{224.8}$
HYB-[Al]-maga39	21.2	$\text{H}_{0.8}(\text{Na}_2\text{O})(\text{Al}_2\text{O}_3)_{1.4}(\text{Si}(\text{CH}_2)_3\text{NH}_2)_{48.8}(\text{SiO}_2)_{181.2}$
HYB-[Al]-maga63	25.5	$\text{H}_{1.2}(\text{Na}_2\text{O})(\text{Al}_2\text{O}_3)_{1.6}(\text{Si}(\text{CH}_2)_3\text{NH}_2)_{36.5}(\text{SiO}_2)_{106.5}$
HYB-[Al]-maga72	25.8	$\text{H}_{17}(\text{Na}_2\text{O})(\text{Al}_2\text{O}_3)_{9.5}(\text{Si}(\text{CH}_2)_3\text{NH}_2)_{236.3}(\text{SiO}_2)_{679.7}$
HYB-[Al]-maga99	30.8	$\text{H}_{52.6}(\text{Na}_2\text{O})(\text{Al}_2\text{O}_3)_{27.3}(\text{Si}(\text{CH}_2)_3\text{NH}_2)_{932.9}(\text{SiO}_2)_{2096.2}$

*calculated by ICP-OES and $\text{Si}_T/(\text{Si}_T + \text{Si}_Q)$ ratio obtained by ^{29}Si -MAS-NMR.

Table S4. Specific surface area (S_{BET}), pore volume (V) and pore diameter (D) of the HYB-magaX and HYB-[Al]-magaX.

	S_{BET} (m ² /g)	V^* (cm ³ /g)	D^* (nm)
Magadiite	25	0.16	19.3
γ -maga28	74	0.36	5.7
PILC-maga28	512	1.1	9.8
HYB-maga28	61	0.24	4.9
HYB-maga61	49	0.19	5.2
HYB-maga88	49	0.19	5.4
HYB-maga100	47	0.23	5.2
[Al]-magadiite	32	0.14	18.0
γ -[Al]-maga39	67	0.40	6.3
PILC-[Al]-maga39	641	1.2	6.8
HYB-[Al]-maga39	60	0.23	5.3
HYB-[Al]-maga63	47	0.17	4.8
HYB-[Al]-maga72	38	0.14	4.3
HYB-[Al]-maga99	40	0.14	5.0

*NLDFT

Table S5. Results of CO₂ adsorption in modified magadiite and [Al]-magadiite.

	-NH₂ groups content^a n_N(mmol)/g of solid	CO₂ adsorption^b (mmol CO₂/g of solid)	Efficiency^c (n_{CO₂}/n_N)}
γ-maga28	0.276	0.101	0.37
HYB-maga28	0.220	0.131	0.60
γ-[Al]-maga39	0.232	0.106	0.46
HYB-[Al]-maga39	0.196	0.128	0.65
Maximum adsorption ^d	-	-	0.50

^a calculated by CHN; ^b measured by TPD;

^c ratio between (CO₂ adsorption)/(-NH₂ groups content)

^d according to the stoichiometry (2 R-NH₂ + CO₂ → R-NH₃⁺ + R-NHCOO⁻)

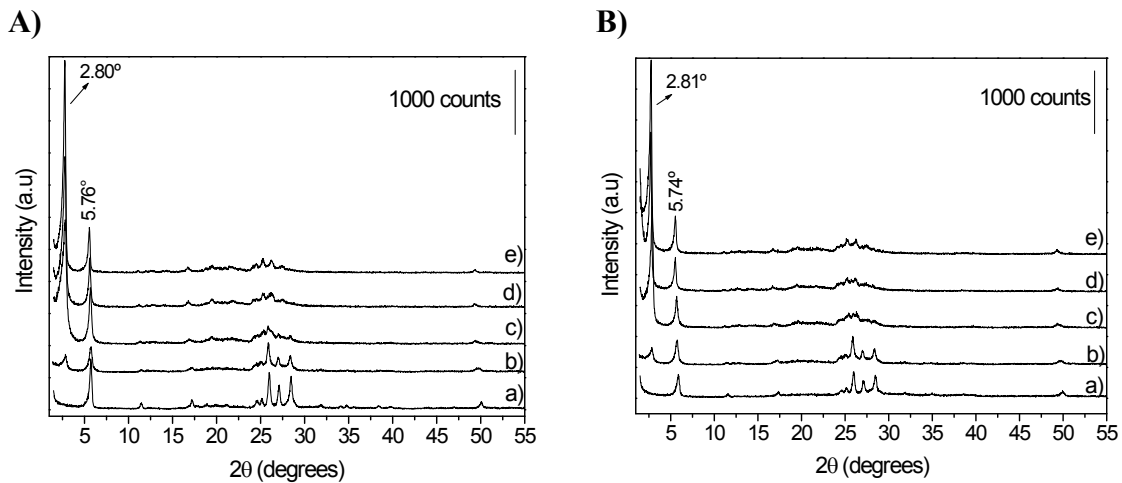


Figure S1. X-ray diffractograms of (A): a) magadiite, b) CTA-maga28, c) CTA-maga61, d) CTA-maga88 and e) CTA-maga100. (B): a) [Al]-magadiite, b) CTA-[Al]-maga39, b) HYB-[Al]-maga39, c) CTA-[Al]-maga63, d) CTA-[Al]-maga72 and e) CTA-[Al]-maga99.

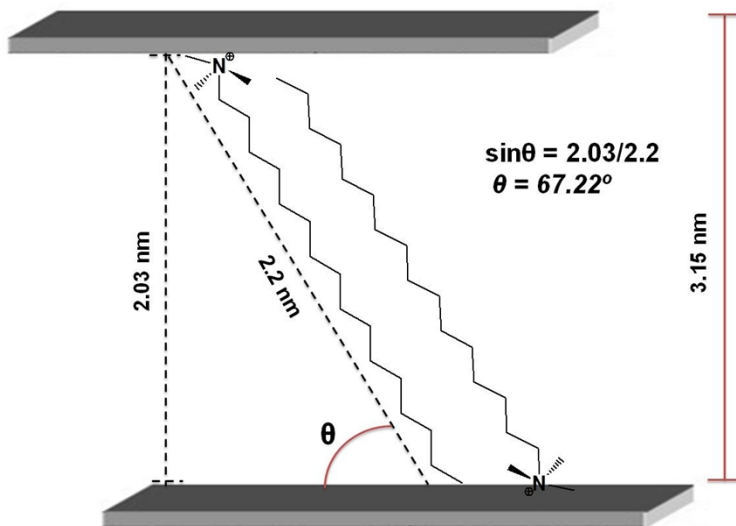


Figure S2. Inclination of CTA⁺ chain in relation to the lamella (magadiite lamella thickness = 1.12 nm^{4,5}).

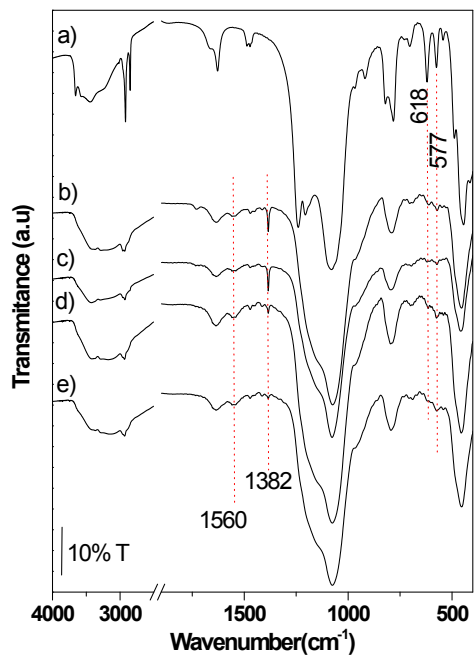
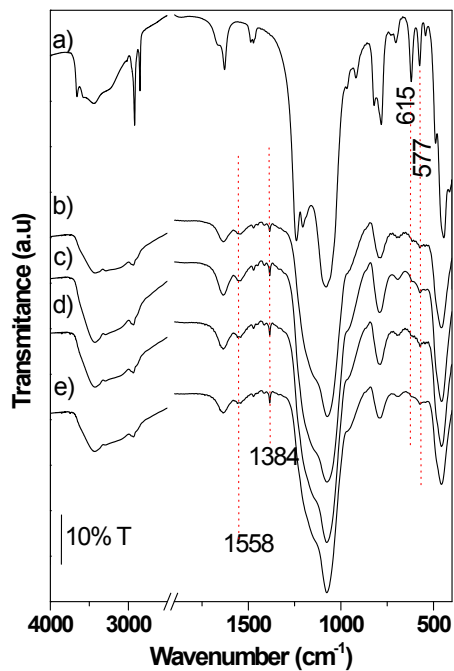
A)**B)**

Figure S3. FT-IR spectra of hybrid materials derived from magadiite (A): a) CTA-maga28; b) HYB-maga-28; c) HYB-maga61; d) HYB-maga88 and e) HYB-maga100. B) FT-IR spectra of hybrid materials derived from [Al]-magadiites: a) CTA-[Al]-maga39; b) HYB-[Al]-maga39; c) HYB-[Al]-maga63; d) HYB-[Al]-maga72 and e) HYB-[Al]-maga99.

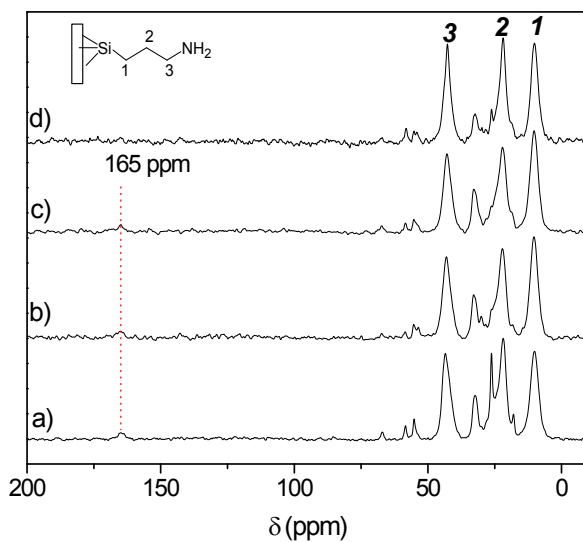
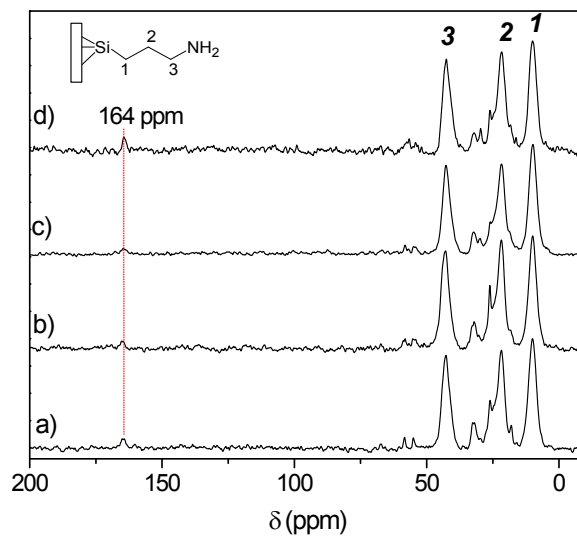
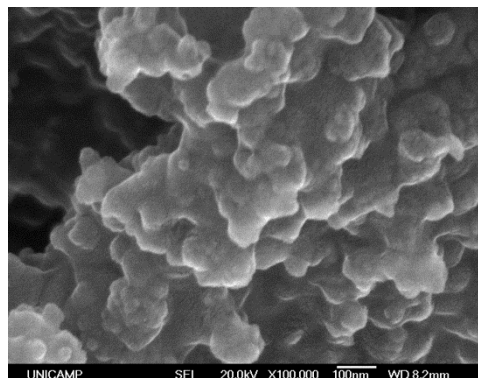
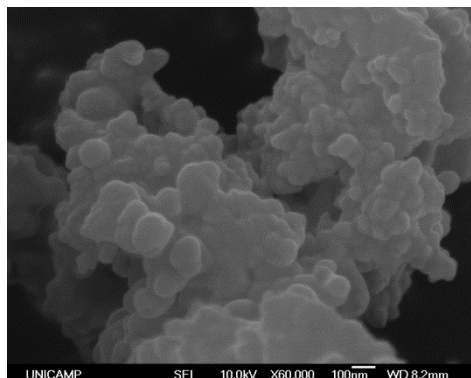
A)**B)**

Figure S4. ^{13}C - $\{^1\text{H}\}$ CP MAS NMR spectra of hybrid materials derived from magadiite (A): a) HYB-maga-28; b) HYB-maga61; c) HYB-maga88 and d) HYB-maga100. B) ^{13}C - $\{^1\text{H}\}$ CP MAS NMR spectra of hybrid materials derived from [Al]-magadiites: a) HYB-[Al]-maga39; b) HYB-[Al]-maga63; c) HYB-[Al]-maga72 and d) HYB-[Al]-maga99. The signals not assigned are due to the presence of residual CTA^+ groups not completely eliminated, as already observed in Figure 4.

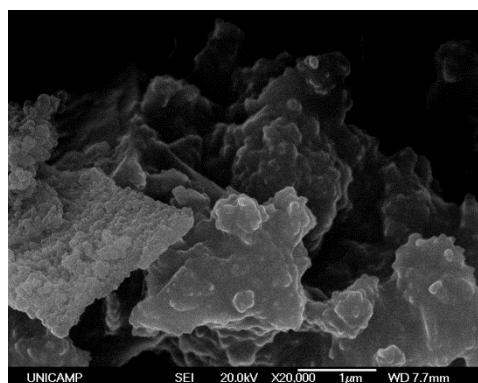
HYB-[Al]-maga39



HYB-[Al]-maga72



HYB-[Al]-maga63



HYB-[Al]-maga99

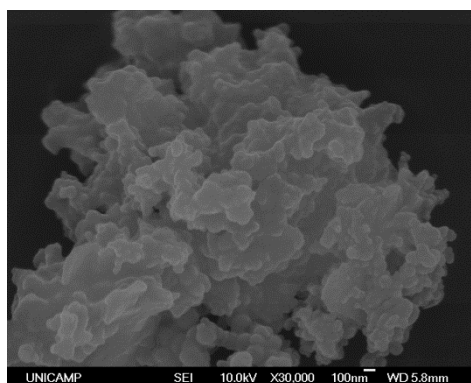
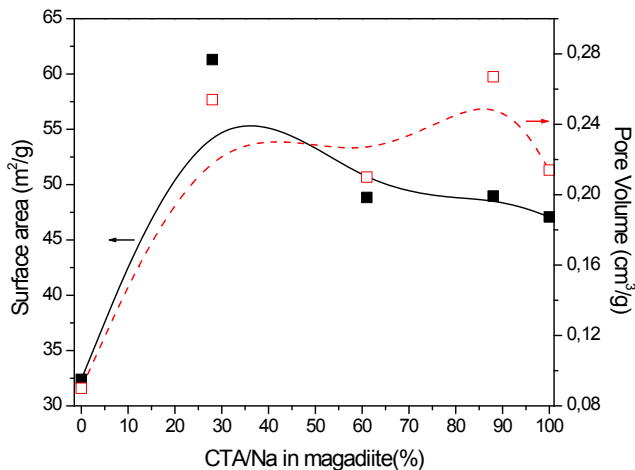


Figure S5. Scanning Electronic Microscopy (SEM) of hybrid materials based on [Al]-magadiite.

A)



B)

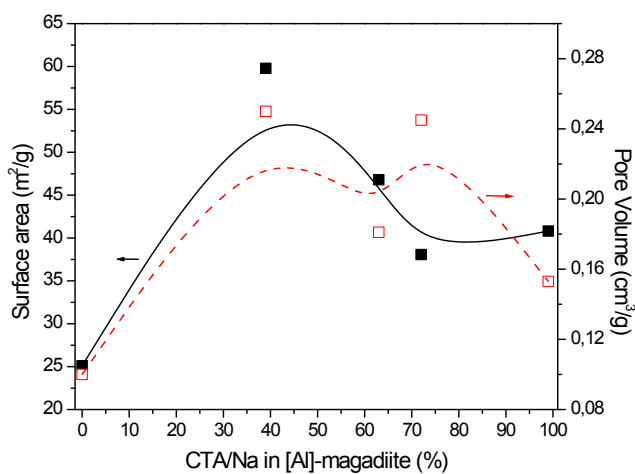


Figure S6. Surface area (■) and pore volume (□) as a function of CTA/Na in magadiite (A) and [Al]-magadiite (B). The lines are only guide for the eyes.

¹ H. Y. Zhu, Z. Ding, C. Q. Lu and G. Q. Lu. *Appl. Clay Sci.*, 2002, **20**, 165.

² H. M. Moura, F. A. Bonk and H. O. Pastore. *Eur. J. Mineral.*, 2012, **24**, 903.

³ S. F. Wang, M. L. Lin, Y. N. Shieh, Y. R. Wang and S. J. Wang. *Ceram. Int.*, 2007, **33**, 681.

⁴ J. M. S. Silva, G. P., J. Bendall, C. Bisio, L. Marchese and H. O. Pastore. *Phys. Chem. Chem. Phys.*, 2013, **15**, 13434.

⁵ J. S. Dailey and T. J. Pinnavaia, *Chem. Mater.*, 1992, **4**, 855.